

Chapter 2

Equipment

In order to carry out the research programme previously outlined, a wind tunnel model was designed and constructed. The purpose of this chapter is to describe and document that model and its ancillary equipment.

2.1 Wind Tunnel

The wind tunnel used was the 450 kW wind tunnel of the Department of Mechanical Engineering, Monash University. The flow was generated by a constant speed, variable pitch axial flow fan. The tunnel was of the single return, closed circuit type, as shown in figure 2.1. There were two main working sections, of $4\text{ m} \times 3\text{ m}$ and $2\text{ m} \times 2\text{ m}$ cross-sections. In the downstream end of the $2\text{ m} \times 2\text{ m}$ section an insertable section was installed, which reduced the working section to $2\text{ m} \times 1\text{ m}$ (height \times width). The circular cylinder was placed in this working section, spanning the 1 m width.

A contraction from the $2\text{ m} \times 2\text{ m}$ to the $2\text{ m} \times 1\text{ m}$ sections was produced to the profile specified by Borger (1976), and the rapid diffusion required downstream was assisted using a three-vaned diffuser, as shown in figure 2.2. With this arrangement, the maximum available working section airspeeds were about 55 m/s in smooth flow and 45 m/s with turbulence grids installed. In the working section, the total pressure was near atmospheric in smooth flow. Attempts to bring the static pressure to atmospheric by venting the rear of the working section were not successful, and degraded the maximum available speed due to momentum exchange with the surroundings. In the end, the working section was sealed, and plenum boxes were installed where the ends of the model projected through the working section walls to restrict the influx of air. To reduce bending of the working section walls caused by pressure differential, the walls were anchored to 125 mm \times 76 mm R.H.S. beams which spanned between the roof and floor of the tunnel.

Large end plates, designed to the specifications of Stansby (1974) were made from 5 mm hardboard, and mounted from the main walls of the working section on folded thin steel Z-sections. The plates extended $2.5 D$ upstream from the model centreline, $4.5 D$ downstream, and $4.75 D$ above and below. The main section of the cylinder spanned between these plates, but was not connected to them. The 5 mm gap between the end of

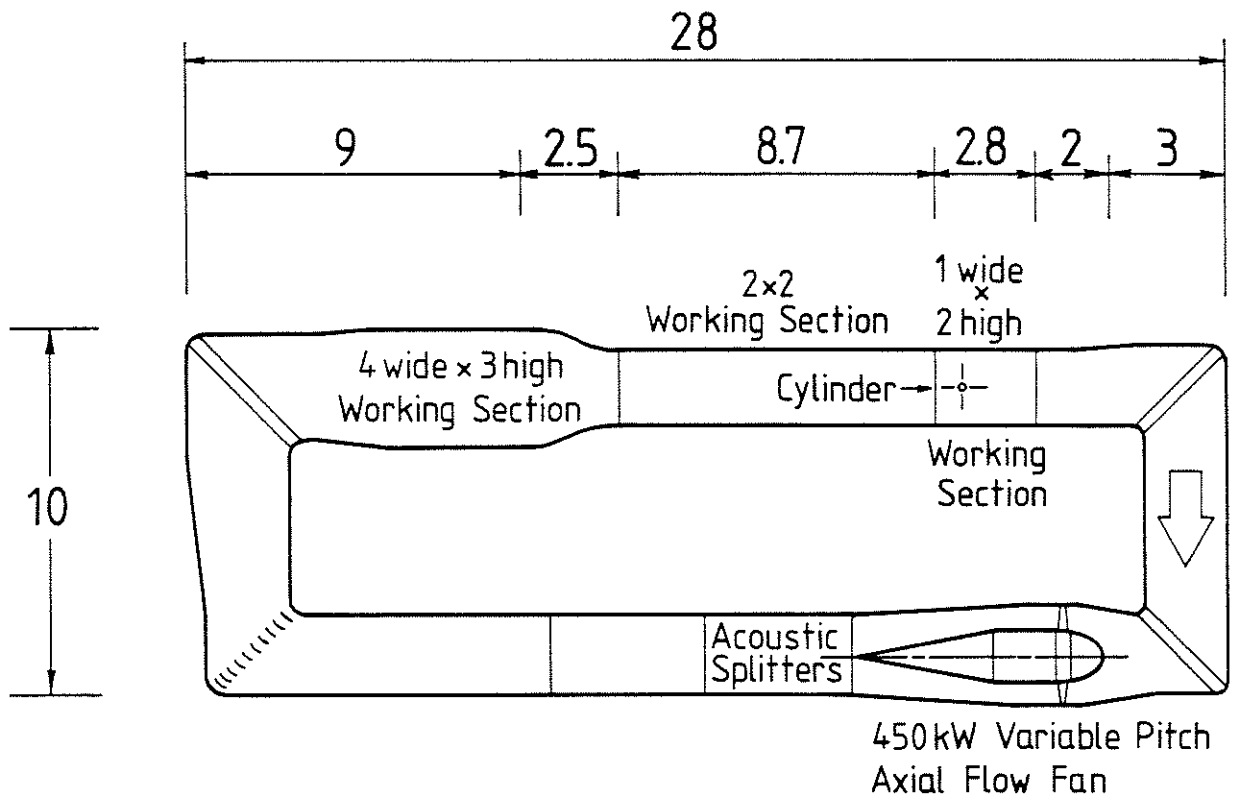


FIGURE 2.1: Monash University 450 kW wind tunnel.

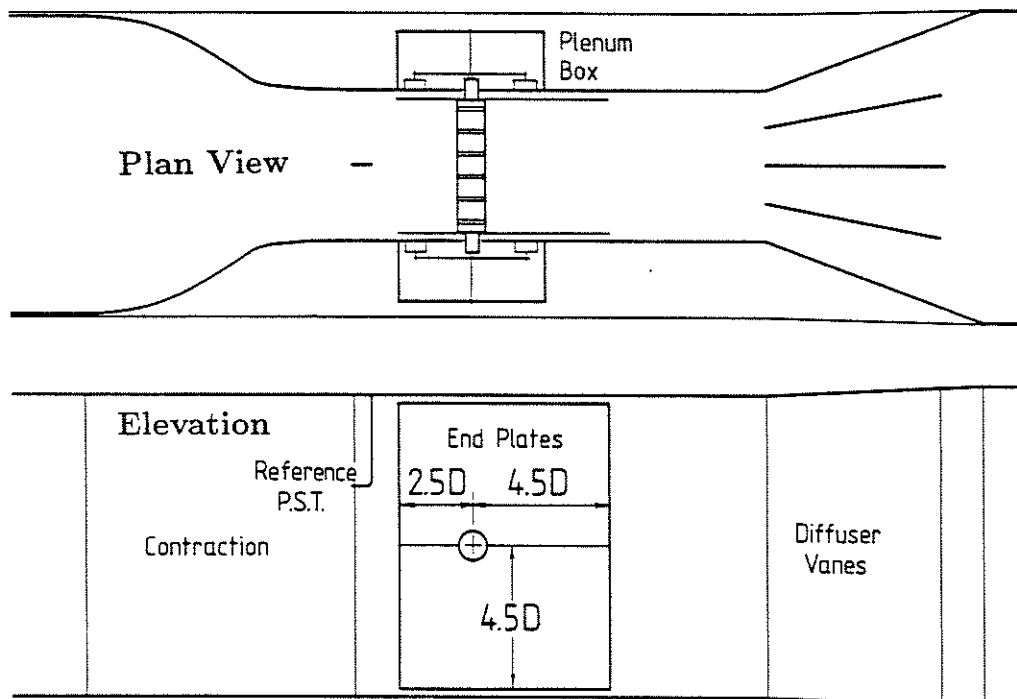


FIGURE 2.2: 2 m x 1 m working section.

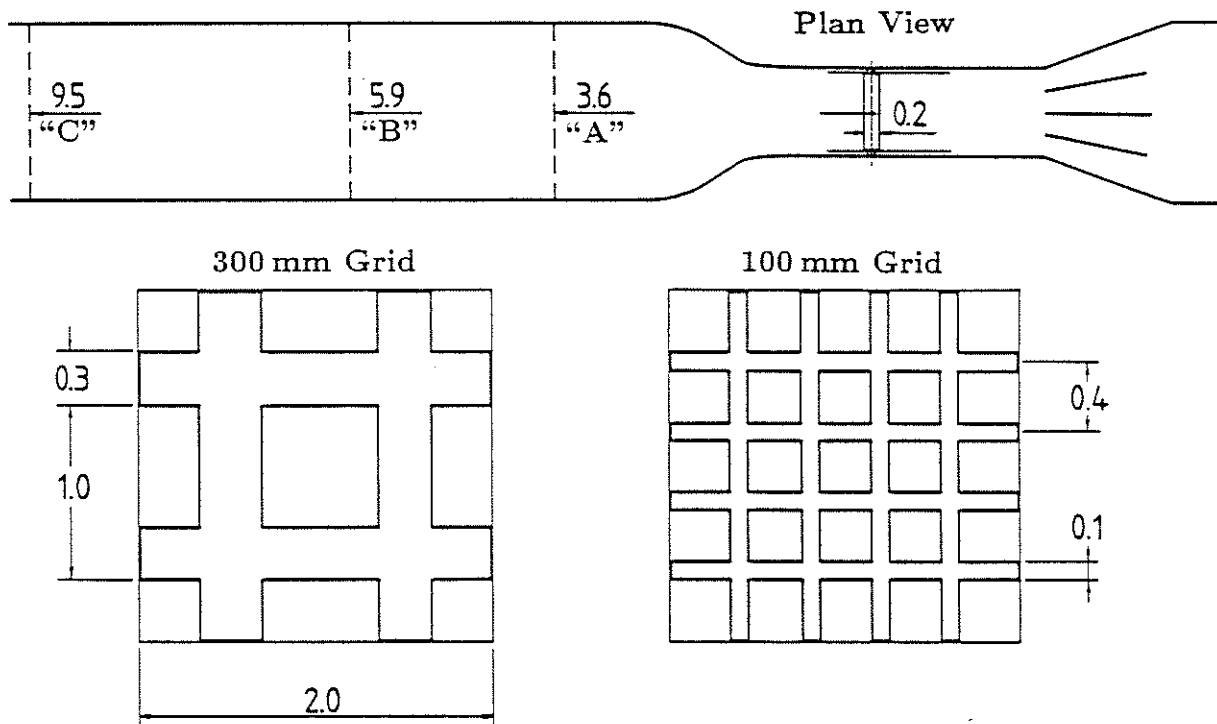


FIGURE 2.3: Turbulence grids and positions.

the main cylinder and the end plates was sealed using synthetic fur, which prevented air flow around the ends of the model, but allowed the model to oscillate in the cross-flow direction. The central section of the cylinder (200 mm diameter), consisting of force transducers and blank aerodynamic sections, was supported on an inner aluminium tube of 101.6 mm diameter, 1.2 mm wall thickness. This inner tube projected through holes in the end plates, through the walls of the working section, and into plenum boxes mounted on the outside of the working section walls, as indicated in figure 2.2.

Also shown in figure 2.2 is the position of a reference Pitot-static tube which was connected to a Betz water manometer (0.1 mm divisions). This combination was used in conjunction with a Comark electronic thermometer to monitor mean airspeeds throughout the experimental programme. Correction factors which related the airspeed indicated by the reference Pitot-static tube to the mean airspeed at the model centreline position were found using a hotwire anemometer placed at the model position.

Five flow configurations with varying turbulence characteristics were used in the experiments. For the nominally smooth flow ($I_u = 0.6\%$), aluminium honeycomb and fine wire meshes were installed at the beginning of the $2\text{ m} \times 2\text{ m}$ section of the tunnel. Two planar turbulence grids installed in the $2\text{ m} \times 2\text{ m}$ section of the tunnel were used to provide turbulent flow. The grids and their positions in the tunnel are shown in figure 2.3. The 300 mm slat grid was installed in positions "A", "B" and "C", while the 100 mm slat grid was used in position "B" only. Details of the flow characteristics produced by these five configurations will be given in chapter 3.

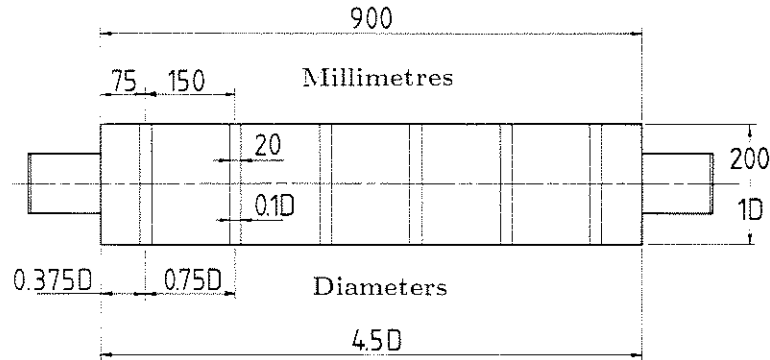


FIGURE 2.4: Drawing of cylinder assembly.

2.2 Cylinder Model

The cylindrical wind tunnel model was of circular cross section and spanned 900 mm between the end plates installed in the working section. The diameter of the cylinder was 200 mm, giving an aspect ratio of 4.5:1 and a blockage of 10%. The model had six force transducer elements, which mounted short—20 mm ($0.1D$) axial length—sections of the cylinder on stiff beam springs to which strain gauges were bonded. Six transducer elements were spaced evenly along the axis of the cylinder, with the remainder of the cylinder being made up of “blank” sections which maintained the cylindrical shape and contained base pressure tapings. The transducer sections and the intervening blanks were mounted onto an inner tube of aluminium which provided structural support. The resulting arrangement is sketched in figure 2.4, and the photograph of figure 2.5 displays the various elements of the cylinder assembly. Small (0.5 mm) axial gaps between the various cylinder segments were sealed using 6 mm wide strips of $30\ \mu\text{m}$ thick

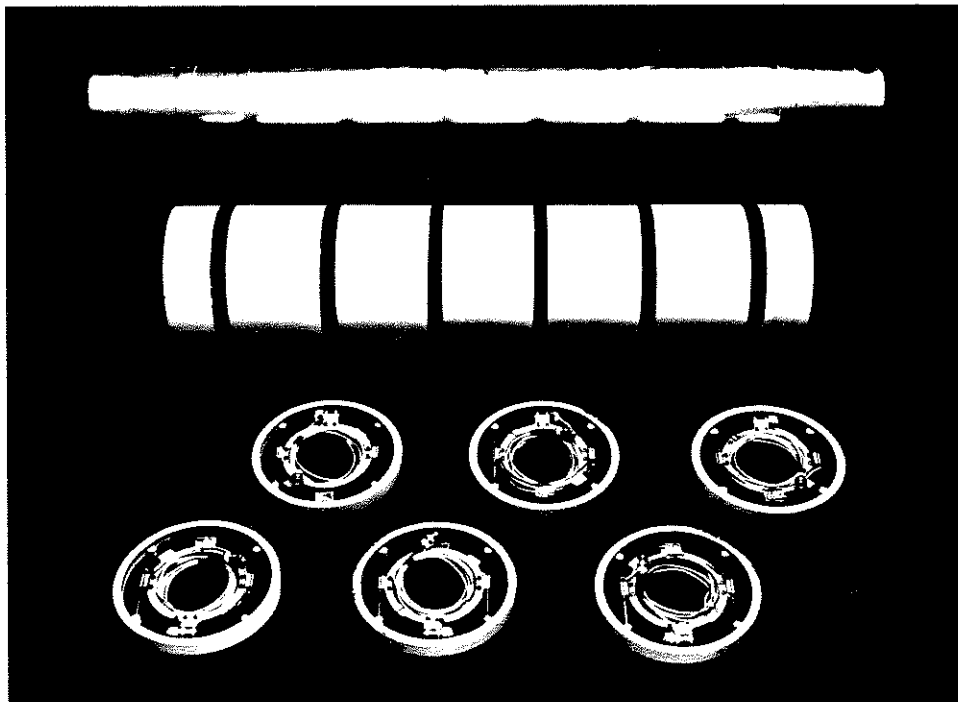


FIGURE 2.5: Components of cylinder assembly.

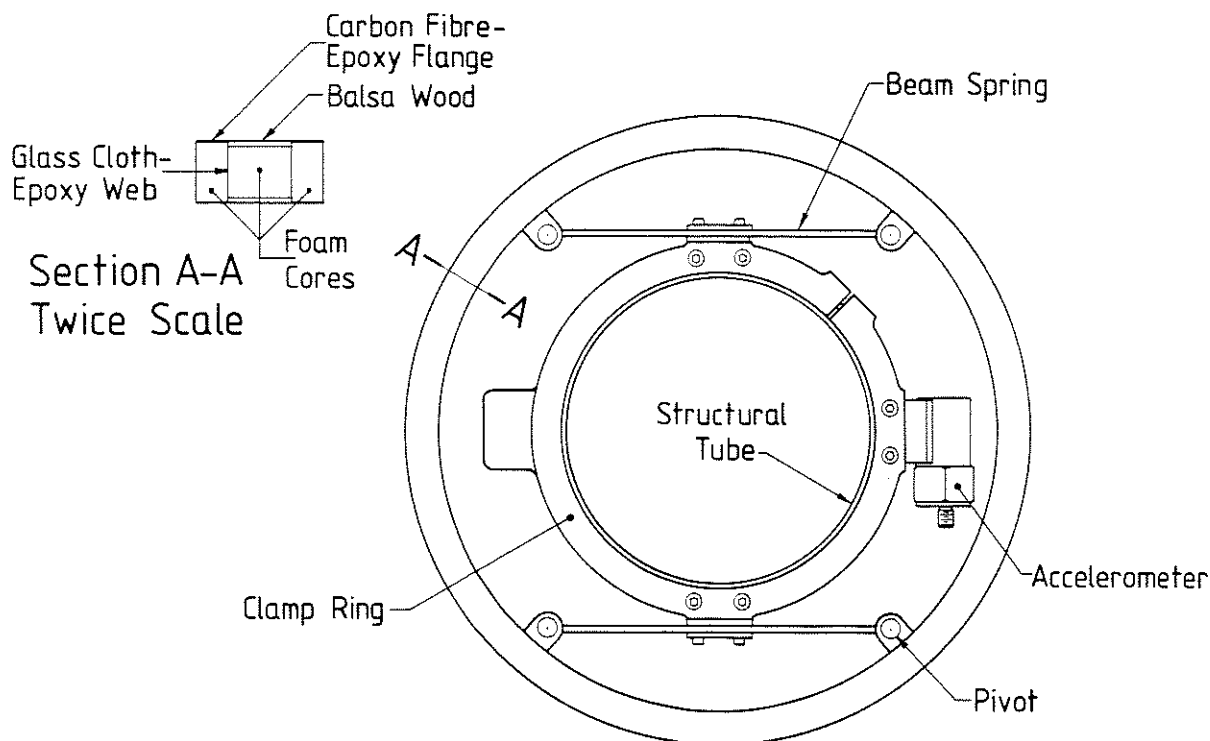


FIGURE 2.6: Force transducer subassembly.

polyurethane elastomer. These were glued to the cylinder segments using pressure pack contact adhesive.

2.2.1 Force Transducers

The force transducers were designed with the objective of measuring cross-flow forces acting on short sections of the cylinder, giving a good approximation to the sectional forces. Short (0.1 diameter axial length) segments of the cylinder were mounted from an inner structural tube on stiff beam springs which had strain gauges bonded to them and connected in a full bridge circuit. Figure 2.6 provides detail of the force transducer assembly and its construction, while figure 2.7 is a photograph of an assembled transducer element. The transducers consisted of an outer cylinder segment, supported from an inner clamp ring of aluminium by phosphor bronze springs to which strain gauges were bonded. The inner clamp ring served to clamp the whole assembly to the structural inner tube and to support the cradle which was used to mount an accelerometer.

The transducers were used to measure forces acting on the cylinder segments while the whole cylinder underwent forced oscillations in the cross-flow direction. These forces were the sum of the aerodynamic forces produced by pressures and shear stresses, and the inertial forces required to accelerate the mass of the segments. Only the aerodynamic portion of the forces was of interest, and the inertial component had to be estimated and removed, as will be described in chapter 4. This had two direct consequences in the design of the transducer assemblies. The first was that the segments of the cylinder mounted on the strain-gauged beams had to be as light and stiff as possible, to minimize the inertial forces and to ensure that any internal resonances were well

above the frequency range of interest. Secondly an accelerometer was mounted at each transducer, so that the local acceleration at the section could be accurately measured.

Construction of Cylinder Segments

The requirements for lightness and rigidity were met by constructing the cylinder segments from carbon and glass fibre composites, foamed plastics and balsa wood. The layout chosen can be seen in the sectional detail provided in figure 2.6. Two ring beams, with carbon-fibre flanges and glass-fibre webs, were glued back-to-back on a spacer consisting of balsa wood and foamed plastics, skinned on the outside with glass cloth. Foamed plastics also provided support to the carbon-fibre flanges of the ring beams, as can be seen in figure 2.7, but most of the shear stiffness came from the glass cloth shear webs. Eight 0.8 mm birch plywood lugs were glued into the segment sub-assembly in pairs at four azimuthal locations. Glass-filled Teflon bushes were pressed and glued into these lugs to provide pivot points between the beam springs and the cylinder segments. The three slices which made up the bulk of each subassembly were cast as longer cylindrical sections inside a machined mould, then removed and slit up. Glass-fibre webs were produced as sheets and glued to the carbon-fibre/foam slices, after which excess material was trimmed off. The three slices were then assembled with epoxy adhesive, together with the plywood lugs, in a jig made from Perspex. Finally, after removal from the jig, any minor gaps were filled and the outside surface was sprayed with epoxy paint and rubbed back to a smooth finish. The completed segments had a mass of 16 gm for a 20 mm long segment of a 200 mm diameter cylinder.

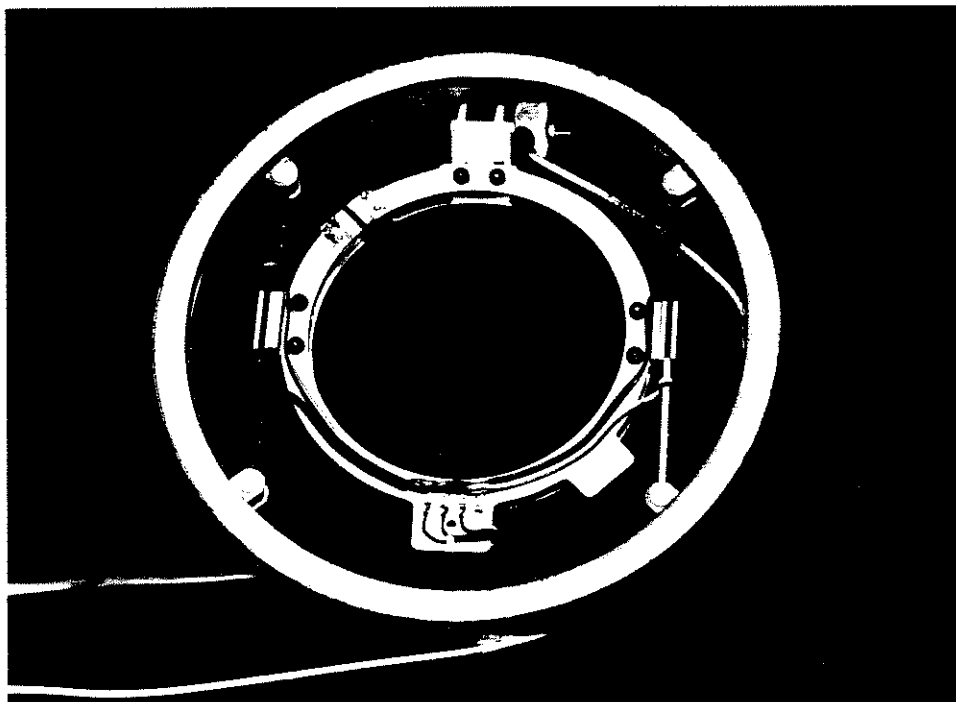


FIGURE 2.7: Force transducer.

Accelerometers

Vibra-Metrics model 1022-LF accelerometers were chosen, and the associated conditioning units were produced at Monash University. The accelerometers were mounted with their axes pointing in the cross-flow direction, strapped to cradles on the transducer clamp rings by nylon cable ties as shown in figure 2.7. The accelerometers were connected to external signal conditioning units by cables which were led out along the axis of the cylinder: these cables can be seen, curled up, in figure 2.5.

The characteristics of the accelerometers were examined by comparing them with a Sundstrand QA-900 servo-accelerometer, which was used as a calibration reference. The low frequency response of the accelerometers was found to be less than ideal, in particular the phase response was not a linear function of frequency. The frequency response functions of the accelerometers and associated digital compensation will be described in Chapter 4.

Sensor Springs and Strain Gauges

The sensor beam springs were fabricated from 2 mm phosphor bronze sheet and had stainless steel tubes soldered to their ends. Music wire pivot pins inserted into these tubes located the ends of the springs between the glass-filled Teflon bushes which were part of the outer cylinder segments.

The springs were designed to be stiff, so that the natural frequency of the outer cylinder segments on the springs would be well above the frequency range of interest in the experiments, which was about 0–100 Hz. After assembly the natural frequency was found to be near 400 Hz, which was considered high enough that the aerodynamic forces measured on the sensors needed no correction for dynamic effects.

As a consequence of the stiffness of the springs, it was decided that semiconductor strain gauges were needed to provide sufficient signal to noise ratio with standard strain bridge amplifier designs. Semiconductor strain gauges have two main disadvantages when compared to standard foil gauges, apart from the higher cost: thermal drift (due to the high gauge factors and temperature variations in the material to which they are bonded) and slight nonlinearity of gauge factor with strain.

In this application it was felt that the temperature drift was not significant, since only fluctuating—not mean—values were of interest. This meant that mean values would be removed before processing, and any change in mean value during the duration of a data record (~40 s) would be small. As an added precaution, the interior of the model was sealed from the external flow, to reduce internal air currents and hence temperature variation. Since the gauges were assembled in a full bridge configuration—one on each spring—nonlinear effects would cancel out if the gauges all had similar characteristics and the same force was applied to the end of each spring. It was assumed that the four gauges in each transducer were similar since they all came from the same production batch.

Kuhlite type ACP-120-300 gauges were selected and bonded to the springs using Micro-Measurements M-Bond 610 epoxy cement. The gauges in each transducer were wired together in a full bridge configuration, and connected to external strain bridge

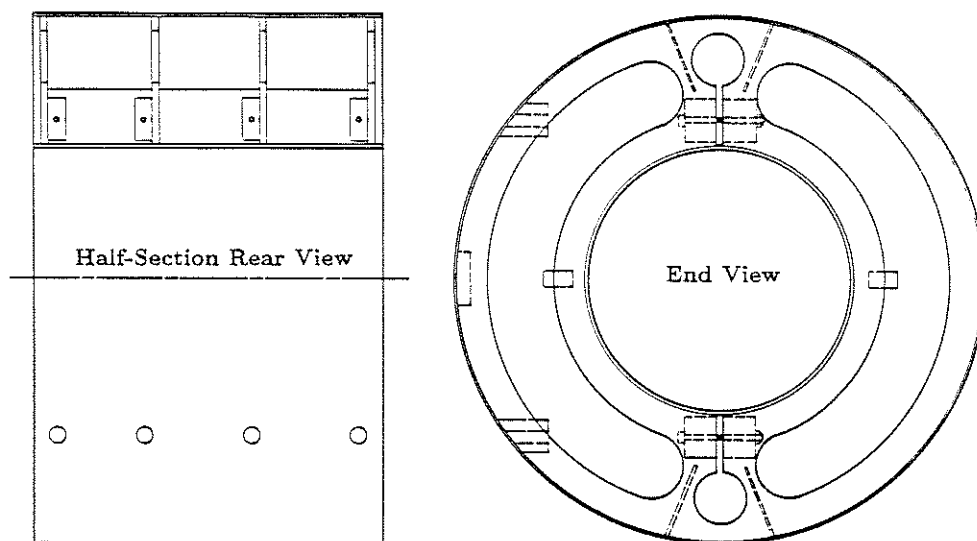


FIGURE 2.8: Blank section subassembly.

amplifiers through cables which were led out along the axis of the cylinder. One of these cables and the associated wiring within the transducer assembly is visible in figure 2.7. The strain bridge amplifiers were produced at Monash University.

Interaction Effects

The mechanical arrangement of the springs and gauges provided a sensor element which was only sensitive to cross-flow force. Measurements showed the transducers to be about 150 times more sensitive to cross-flow than streamwise force.

The transducers were found to have a slight sensitivity to applied moments. When it was arranged so that cross flow force was applied at one cylinder radius from the centreline, output changed by about one-sixtieth of the full reading found when the force was applied at the model centreline. This moment sensitivity was due to the transducer outer segments being less than perfectly rigid, so allowing the applied force to be distributed in unequal proportions to the four internal beam springs.

No interaction corrections were made for either streamwise forces or moment effects, due to the comparative insensitivity to these loads.

2.2.2 Blank Sections

The blank sections which were placed between the transducer segments were constructed of birch plywood and balsa wood so that they would be light and stiff. Construction of the blanks is indicated in figure 2.8. They contained base pressure tapings of 1.2 mm I.D. and had 6 mm holes situated in the wake region which gave access to clamping screws; these access holes were covered with adhesive tape after cylinder assembly. The base pressure tapings were connected to a T.E.M. Instruments Ltd. multiple tube inclined manometer, located outside the wind tunnel, by 1.5 mm bore plastic tubes, which were led out of the model down the cylinder axis.

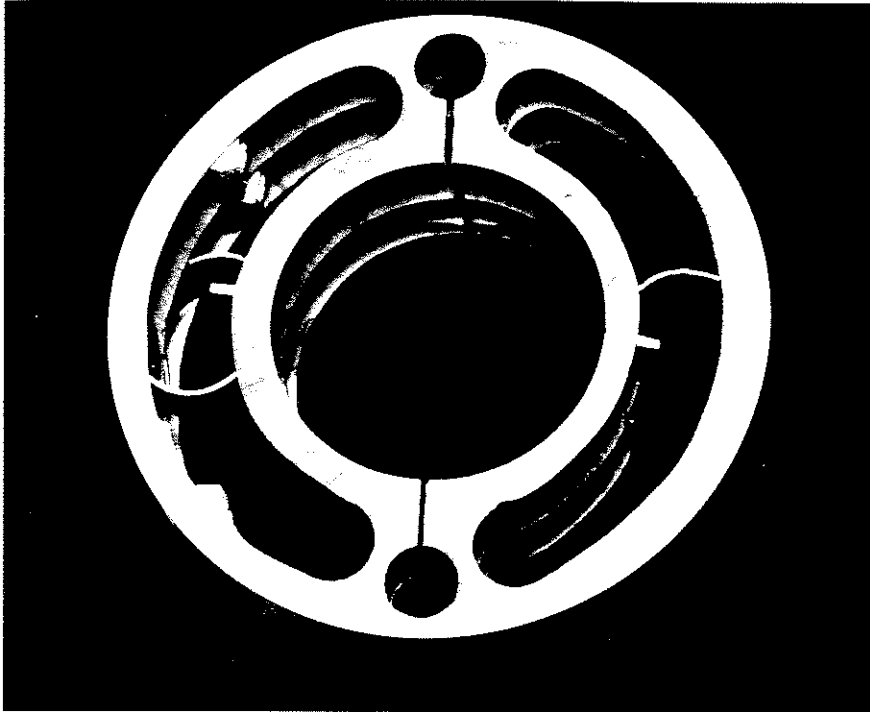


FIGURE 2.9: Completed blank section.

gluing it in position. After the glue had dried, the blanks were sanded down and filled where required to ensure a cylindrical shape, then covered with light glass cloth and epoxy, and again sanded to shape. Finally they were sprayed with epoxy paint and rubbed back to a smooth finish. A completed section is shown in figure 2.9.

2.2.3 Dimensional Accuracy

After assembly of all the segments on the inner structural cylinder, dimensional accuracy was checked by mounting the assembly between centres and taking measurements with a dial gauge at 25 axial locations along the cylinder. At each axial station, readings were recorded at 10° increments. The readings were transferred to a computer, and circles of best fit were computed for each station: see figure 2.10 for example. These circles enabled the cylinder diameters and the amount of radial runout (variation in radius) at each station to be assessed. The maximum runout found was 0.2 mm or 0.1% of diameter; the average maximum runout was 0.15 mm. The average cylinder diameter was 200.5 mm, with a standard deviation of 0.12 mm.

Inevitably there were some discontinuities in the shape, such as where a transducer segment was butted up to a blank section, where there might have been a step change of radius of as much as 0.3 mm on the basis of the average maximum runout value quoted above. The gap between each segment of the cylinder also provided a discontinuity. The gap of ~ 0.8 mm was covered with thin ($30 \mu\text{m}$) polyurethane elastomer, but since it was wrapped around the cylinder under slight tension (to avoid wrinkling), it tended to sag slightly in the gap. The discontinuity in radius and surface roughness provided by the polyurethane film was felt to be unimportant compared to that caused by the gap itself.

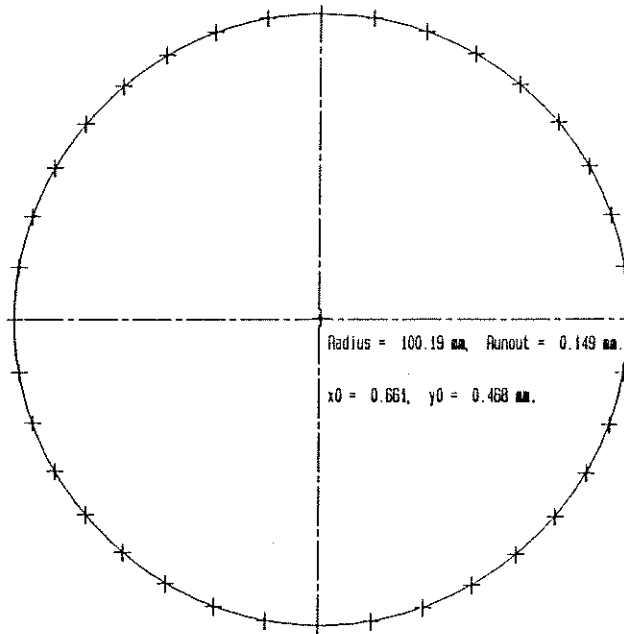


FIGURE 2.10: Measurements at one axial station and fitted circle.

gap itself.

The effects produced by irregularities of shape were not directly assessed in the experimental programme.

2.2.4 Assembled Cylinder

Two photographs of the assembled cylinder installed in the wind tunnel are presented in figures 2.11 and 2.12.

The photograph of figure 2.11 was taken looking downstream towards the model. In this view the large (black) endplates mounted on folded steel sections can be seen standing proud of the main working section walls (white). The six transducers and the seven blank sections are clearly seen. Between the left-hand end of the cylinder and endplate is synthetic fur (black and white) used to seal that air-gap. Downstream of the model at the end of the working section are the three diffuser vanes. The reference Pitot-static tube can be seen in the top foreground.

Figure 2.12 gives the view upstream from behind the model. Immediately evident are the access holes at the rear of the blank sections. In fact, these holes were covered with clear adhesive tape, and since they were located downstream of the first separation point, the minor discontinuity was thought to have little effect. Past the model can be seen the end of the contraction (grey) from the $2\text{ m} \times 2\text{ m}$ section to the working section, and then the larger of the two turbulence grids used in the experiments, which was in position "B".

In both views the smooth polished surface of the cylinder is evident.

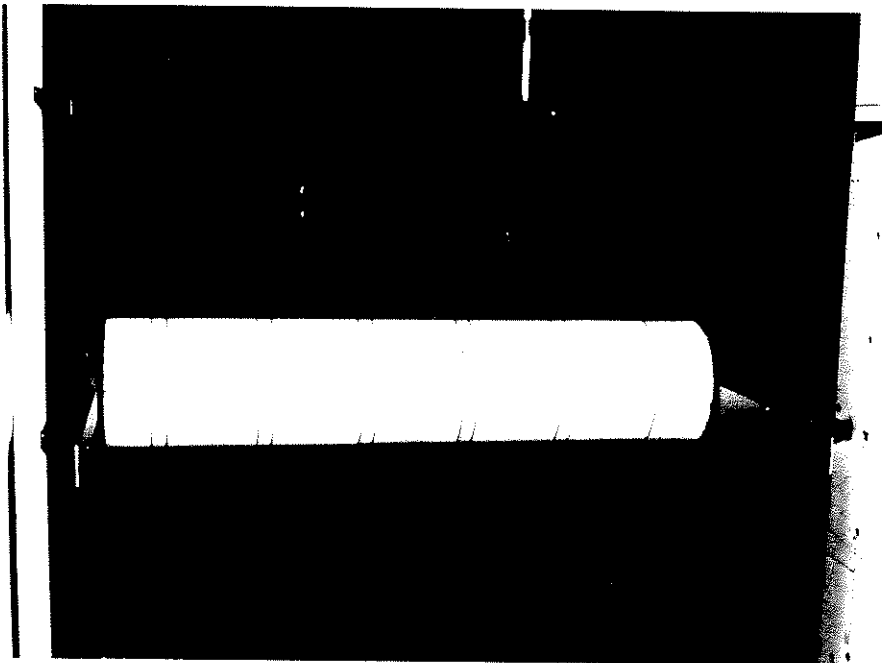


FIGURE 2.11: A view of cylinder installed in working section, looking downstream.

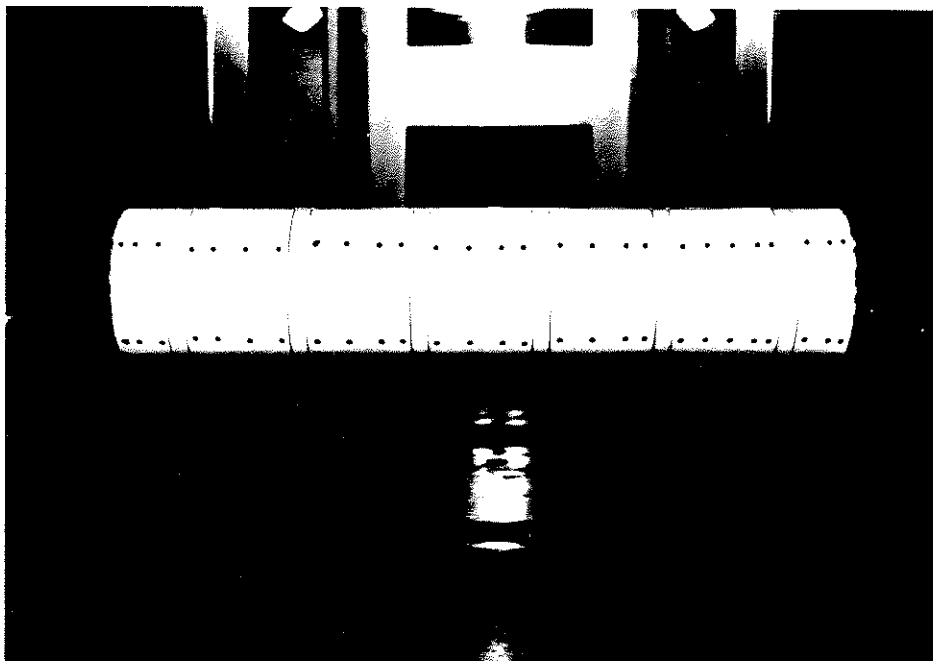


FIGURE 2.12: The view upstream from behind the cylinder.

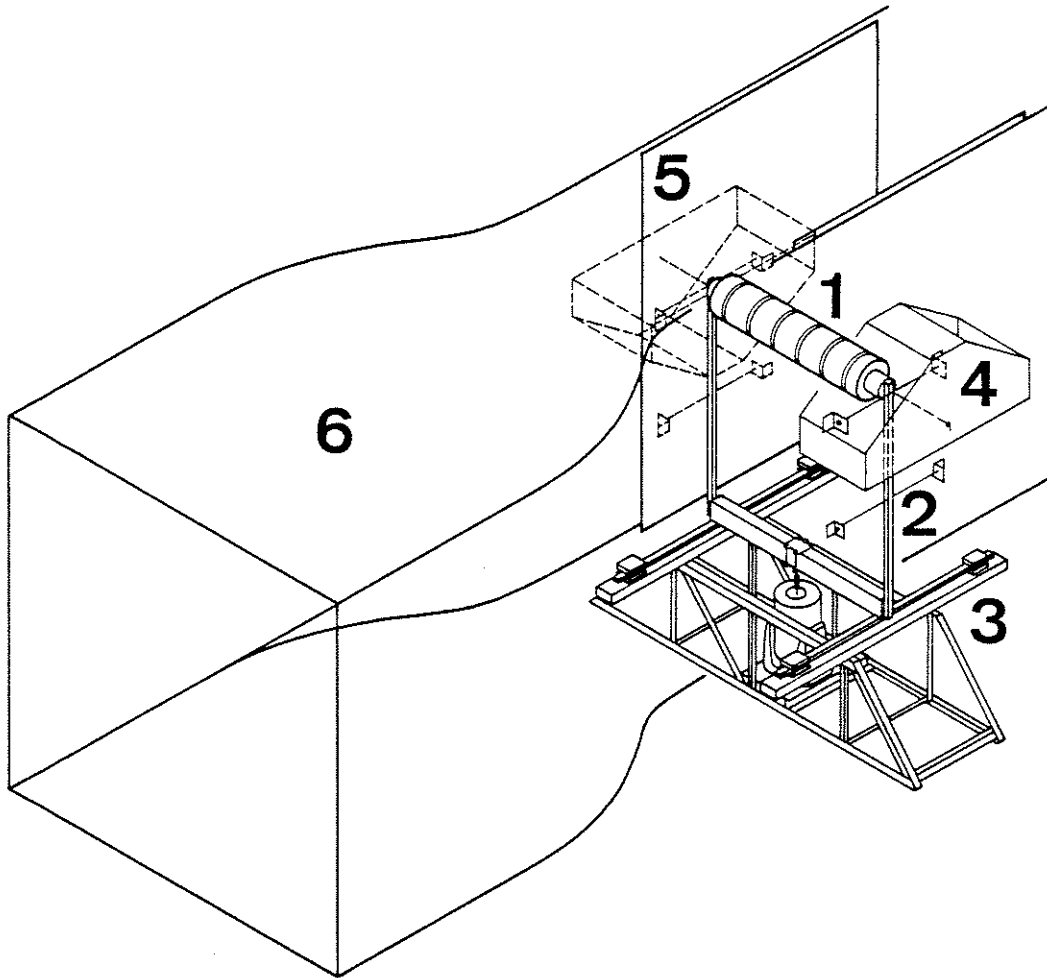


FIGURE 2.13: Isometric sketch of model installed in working section. 1; Cylinder model. 2; Rectangular aluminium tube yoke. 3; Beam springs and truss assembly. 4; Plenum box. 5; End plate. 6; Contraction.

2.3 Cylinder Support and Oscillation System

The part of the model described so far occupied the wind tunnel working section. Outside this, the model was supported and guided by a combination of a rectangular aluminium tube yoke and a harness of taut music wires which constrained motion to the cross flow direction. Underneath the tunnel floor, the yoke was clamped to two steel R.H.S. beam springs, and the whole assembly was driven up and down at its resonant frequency by an electromagnetic shaker. The frequency could be varied by adjusting the length or changing the cross-section of the beam springs. A steel truss assembly was manufactured to hold the shaker and the ends of the steel beam springs. The main elements of the system just described can be seen in the isometric sketch of figure 2.13.

The next two figures show the model set up in a dummy wooden jig, built to represent the working section of the wind tunnel. This set up was useful in the development of the model and the transducers, calibration system and data reduction.

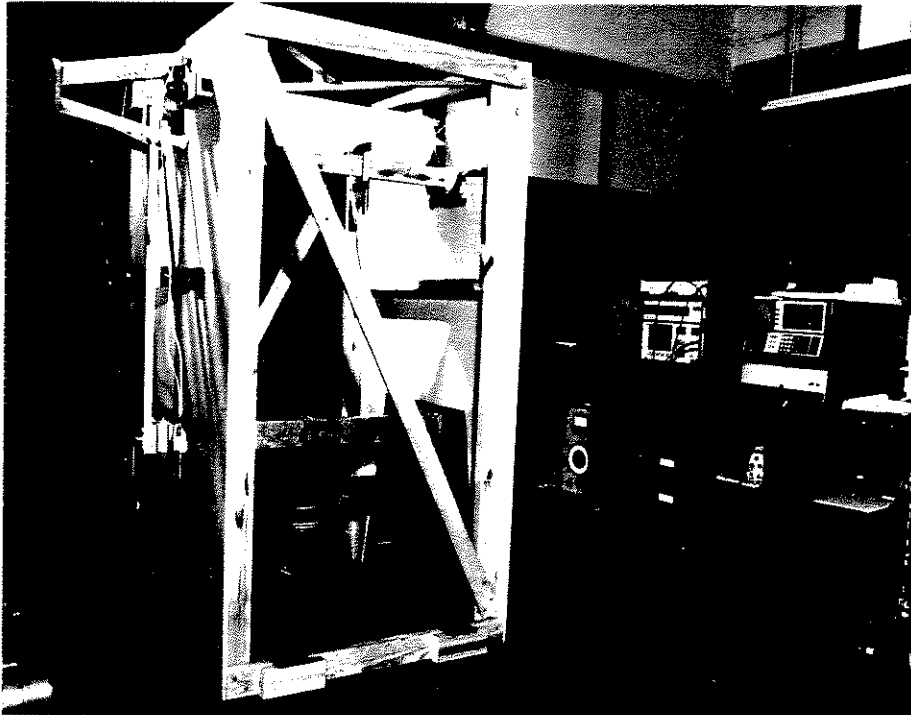


FIGURE 2.14: Model installed in development rig.

Figure 2.14 shows a view of the whole development rig. The red-painted steel truss which held the shaker and beam springs was here bolted down to the hard-floor in the Dynamics Research Laboratory. The cylindrical device sitting in the centre of the truss is the electromagnetic shaker. The white cylinder model can be seen in the centre-top of the wooden jig. The inner aluminium tube projects through holes in the sides of the jig (which represent the walls of the wind tunnel working section) and is connected to the yoke, constructed from rectangular section aluminum tube. This runs down the walls of the jig and across the top of the truss and shaker. The beam springs which supported the yoke assembly were changed after this photograph was taken, and will be shown in more detail in figure 2.17.

The stool-like device attached to the outer wall of the jig serves to hold the outer end of one of the music wire guides. These guides and the connection between the cylinder and the support yoke are more clearly seen in figure 2.15. Figure 2.15 gives an end-view of the cylinder held in the jig of figure 2.14. The internal construction of the cylinder blanks can be seen together with accelerometer and strain bridge cables, and base pressure-tapping tubes. Just visible inside the model is one of the accelerometers. The vertical square-section yoke tube is seen bolted to a turned aluminium cap which was epoxied inside the end of the cylindrical support tube. Let into this tube, at the centre of the cap, is an aluminium block, held in place with four bolts. Music wire guides pass through a turned post in the centre of the block and were clamped with grub screws, located in the post. The wire which runs left-to-right in this figure restrained the cylinder from moving fore and aft along the tunnel, and supported drag loads experienced by the cylinder (assisted by an additional clamp placed on the right-running wire). The wire which runs along the model centreline provided axial restraint.

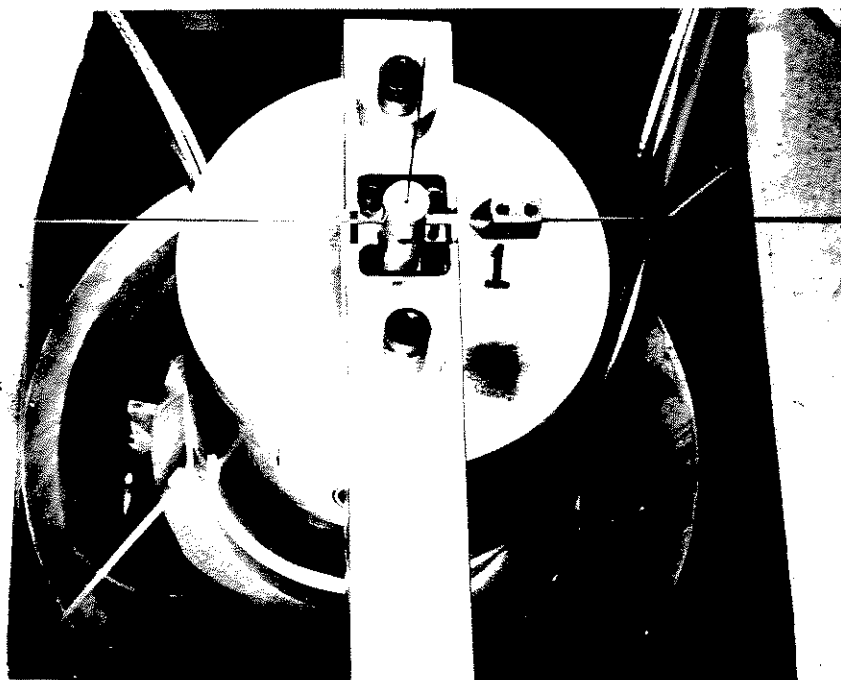


FIGURE 2.15: End view of model in development rig.

As well as these sets of guide wires, there was an additional set to brace the middle of the vertical struts of the yoke in the fore-and-aft direction. This suppressed an unwanted vibration mode which was found in the development set-up, and subsequently verified by computational modal analysis.

2.4 Plenum Boxes

The ends of the structural inner aluminium tube which supported the cylinder sections projected through holes in the working section walls and into plenum boxes which prevented air from flowing into the working section. Figure 2.16 is a photograph showing the inside of one of the boxes. The end of the structural tube and the top of one of the yoke struts were contained in the box; the strut passed through the lower face of the box and the surrounding gap reduced to a minimum with adhesive tape. Strain bridge and accelerometer cables from three transducers can be seen, as can all the pressure tapping tubes and the music wire guides. The top faces of both boxes had Perspex covers, here removed for access.

2.5 Suspension Springs

The cylinder-yoke assembly was supported from beneath the floor of the working section on beam springs. The natural frequency could be varied in the range 10 Hz–60 Hz by varying the length or cross-section of the springs. Figure 2.17 is a photograph of one of these springs on its mounting. The lower end of the yoke is clamped to the centre of the (blue) spring, which was a 1400 mm length of 51 mm × 25 mm × 3.2 mm 350 Grade

R.H.S. The ends of the springs had roller supports, made from ball-races contained in aluminium blocks. These blocks are seen in the photograph with the spring passing through them; they in turn were supported on a more substantial piece of R.H.S. which had slots machined in it to allow the position of the blocks to be changed.

In this photograph the model was installed in the wind tunnel; the support truss was clamped to the floor beams of the Aerodynamics Laboratory.

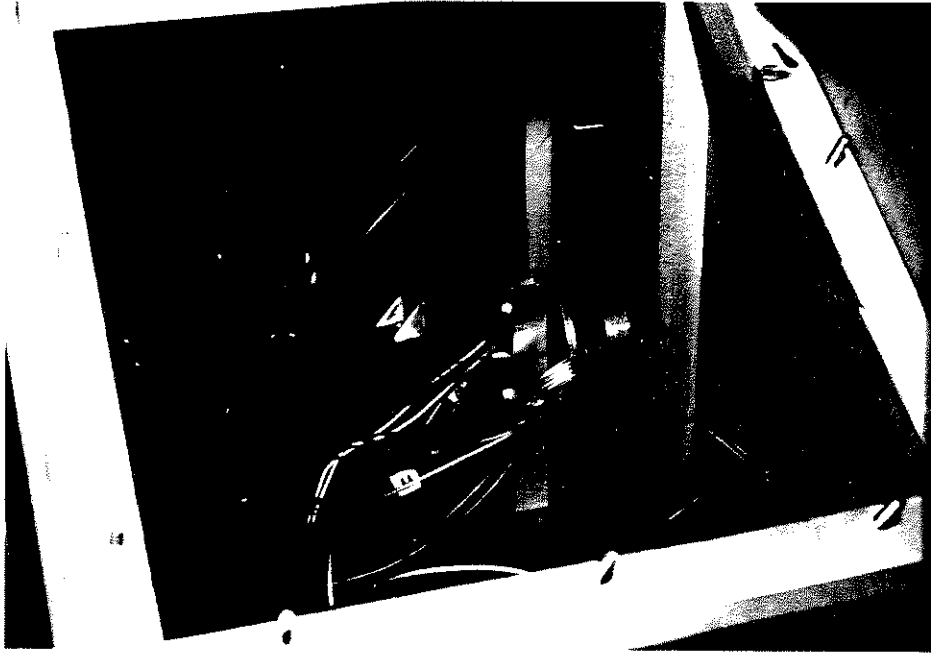


FIGURE 2.16: View inside a plenum box.

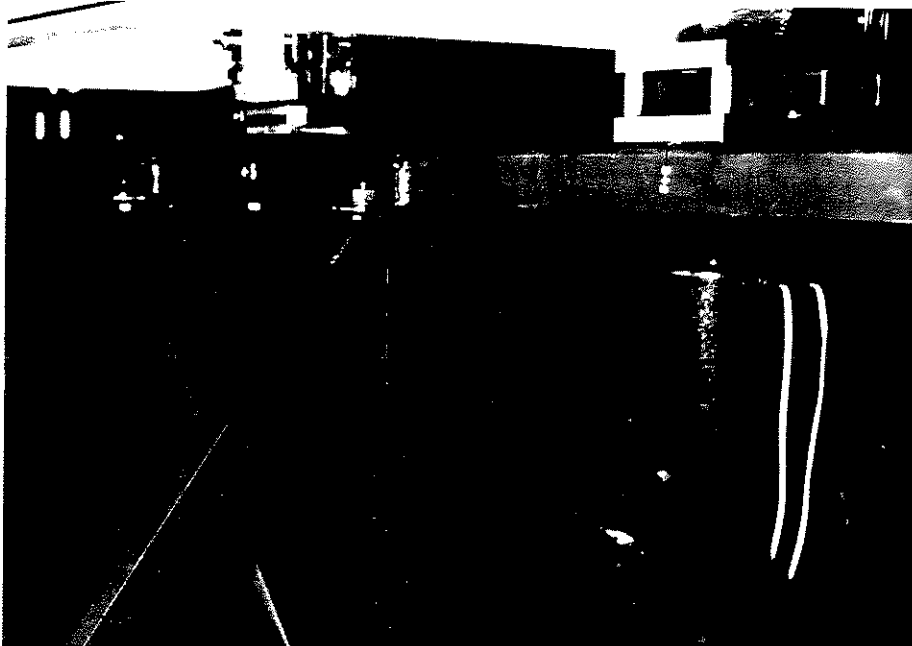


FIGURE 2.17: Beam spring, supports, truss and shaker.

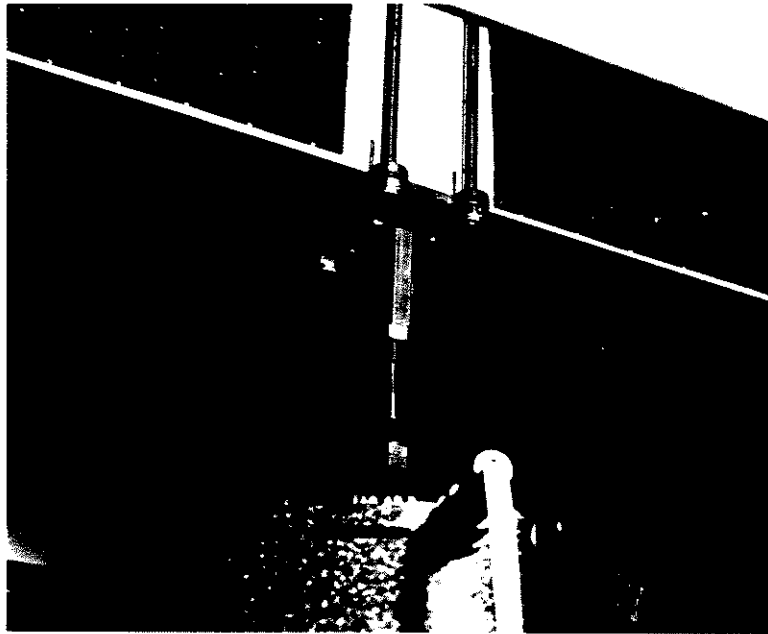


FIGURE 2.18: Connection between shaker and yoke.

2.6 Shaker

The shaker chosen was an MB Electronics type PM-100, which was rated at 100 lbf and had a maximum stroke of 1/2 in. The connection between the shaker and the yoke is shown in figure 2.18. The shaker is positioned beneath the centre of the yoke and the force was transmitted through a length of 1.5 mm diameter music wire. This piece of wire formed part of the quill which can be seen connecting the shaker and the yoke in the photograph.

The shaker was powered by two MB Electronics type 2250MB Power Amplifiers. The signal to the amplifiers was normally provided by a Hewlett-Packard 3311A Function Generator, which could provide sinusoidal signals of adjustable frequency and amplitude. In some instances a random input to the amplifiers was required, in which case a Brüel & Kjær 1040 Sine-Random Generator was used.

2.7 Calibration Set-Up

Initially it was planned to perform static calibration of the force transducers, by fitting a relationship between applied static force and voltage output from the strain bridge amplifiers. This idea was abandoned after it was found that the thin polyurethane film used to seal the air gaps between the segments of the cylinder had slightly visco-elastic properties. Sudden application of a steady load produced a signal which jumped almost instantaneously to about 90% of its steady state value and then relaxed slowly to the full value over a period of several minutes. This meant that the relationship between an applied dynamic load and transducer output was uncertain, so an alternative calibration strategy was developed.

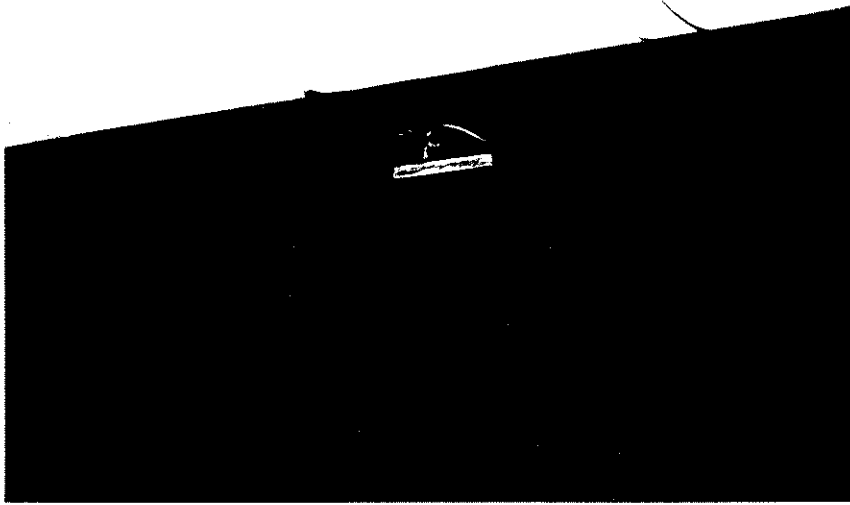


FIGURE 2.19: Load-beam, in place for calibration run, below cylinder.

The appearance of the response to the suddenly applied steady load suggested that two very different time scales effectively governed the behaviour of the polyurethane material, and that response to a rapidly varying load would be essentially elastic. This hypothesis was confirmed by comparing Frequency Response Functions of the transducer strain bridge to applied acceleration computed with and without the presence of the film. The magnitude response was changed (from 2 Hz up to 100 Hz at least) by an approximately constant amount, while the phase response was essentially unaffected. These facts suggest that for dynamic loads the film behaved essentially like a spring acting between the transducer rings and the adjacent blank sections of the cylinder.

The alternative calibration procedure was to load the transducer rings with a small load-beam, and then cause the model to oscillate, thus delivering a time varying load to the transducer. The load-beam, clamped onto a heavy steel stand, is shown in place below the model in figure 2.19. The amount of load could be easily monitored through a set of strain gauges on the load beam and using a static calibration of the beam. The oscillation frequency (~ 15 Hz) was low compared to the fundamental of the beam (70 Hz), and the damping of the load-beam system was light, hence no correction for transmissibility was necessary. The signal from the force transducer, after correction for inertial and other effects, was calibrated to the signal delivered by the load-beam. The good agreement between the two signals provided confirmation of the correct operation of the whole dynamic measurement system. The digital signal processing involved will be described in more detail in chapter 4.

A diagram of the equipment used during calibration is shown in figure 2.20. During calibration, each transducer was connected to the same amplifiers and anti-aliasing filters used for wind tunnel running, and a separate amplifier and filter set was used for the load-beam.

The discovery of the visco-elastic behaviour had the important consequence that the equipment could not be used to measure mean drag loads, which otherwise could

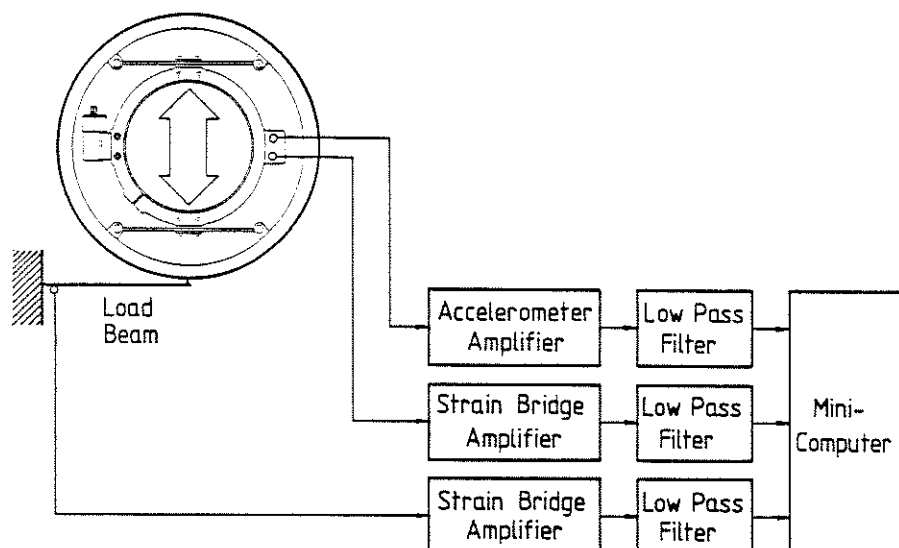


FIGURE 2.20: Schematic showing equipment layout for calibration.

have been accomplished simply by rotating the transducers through 90° on the inner structural cylinder. A number of alternatives were tried in an effort to find a material which would seal the gaps between cylinder segments without significant visco-elastic behaviour. All the alternatives were unsatisfactory, either due to greater visco-elastic effect or a lack of durability in the wind tunnel.

2.8 Data Collection

The cylinder model had six transducers, each of which contained a strain gauge bridge and an accelerometer, so in total there were twelve channels of data to be dealt with. This section describes the arrangements made for analogue conditioning and subsequent digital sampling of these signals. The diagram of figure 2.21 shows the layout of the equipment.

Custom-built amplifier units were used to produce signals from the strain gauge bridges and accelerometers. These signals were then passed through anti-aliasing filters before sampling.

There were not enough matched filters available to deal with twelve channels of data simultaneously, so three sets of four filters were used. Two of the three sets (labelled "Hydro A" and "Hydro B" in figure 2.21) were built at Monash University, while the other set was a Wavetek 816 multichannel filter. All sets contained quasi-Butterworth switched capacitor filters, and had selectable cutoff frequencies, but since the order of the filters varied between the two types, they produced different time delays. These differences were corrected during digital signal processing, to be described in chapter 4.

The twelve channels of data were collected at the same time during each run, since part of the objective was to examine the relationship between the aerodynamic forces at the six transducers. Although the twelve channels could be collected at the same time, the sampling was not simultaneous at each channel, since the analogue-to-digital converter contained one processor, which switched rapidly from one channel to the next

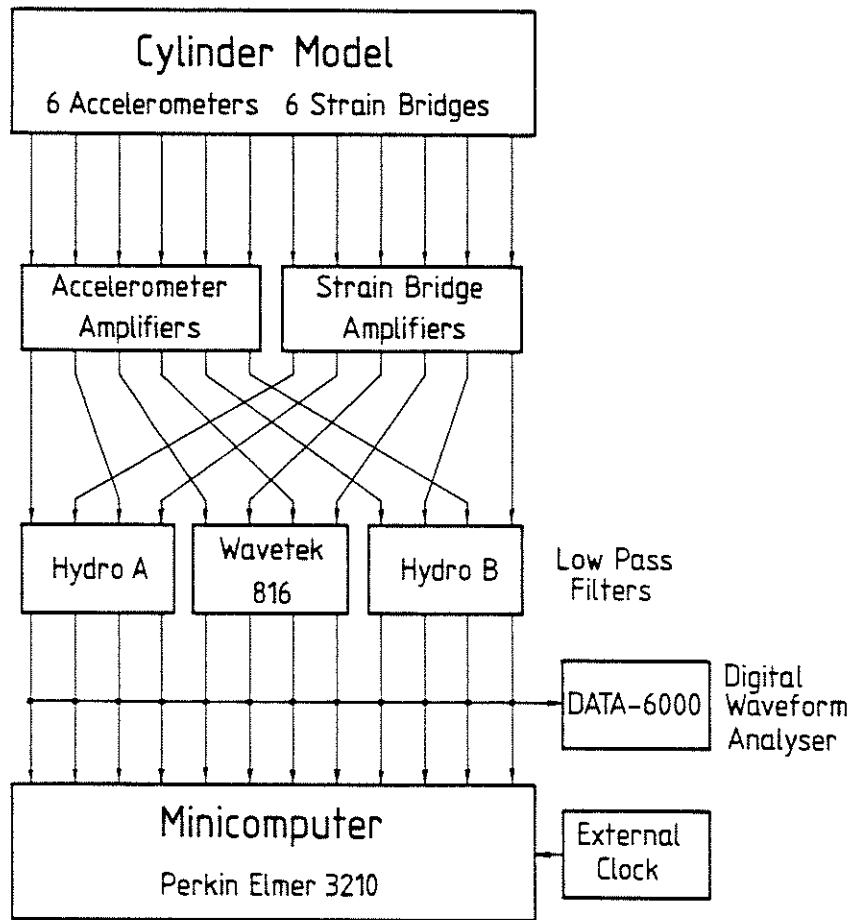


FIGURE 2.21: Schematic of data collection arrangement.

between each signal from the sampling clock source. The subsequent delay from channel to channel was also later corrected during digital processing. The sampling rate of the analogue-to-digital conversion could be set from an external clock source: two sampling frequencies, 200 Hz and 400 Hz, were used. After collection, the sampled data were saved on magnetic tape for later processing.

For monitoring the data collection, a digital waveform analyser could be connected in parallel to the output ports of the anti-aliasing filters.

2.9 Computing Equipment

Digital sampling, storage and processing of data taken from the wind tunnel model was carried out using a Perkin-Elmer 3210 minicomputer, which ran the UNIX operating system. A Data Precision DATA-6000 digital waveform analyser was employed when more immediate processing of data was needed. This was used throughout the experimental programme for monitoring signals and in setting the frequencies and amplitudes at which the model was forced to oscillate. In addition, a Hewlett-Packard 5423A Structural Dynamics Analyser was used in development work and for checking the equipment each time it was installed in the wind tunnel.

2.10 Anemometry Equipment

Mean and fluctuating flow velocities were measured at the model position for the five flow configurations used in the experiments. The measurements were taken without the model installed, since the intention was to describe the oncoming flow. The velocities were measured using the following equipment manufactured by Thermal Systems Incorporated:

- 1054B Constant Temperature Hotwire Anemometer
- 1056 Variable Decade 5:1 Bridge Resistor Unit
- 1051C Correlator

Both single (T.S.I. Model 1241-20) and crossed (Model 1210-20) sensor hotfilm probes were used. The mean and fluctuating voltages produced by the equipment were measured using the DATA-6000 waveform analyser. When velocity spectra were required, linearized anemometer output was low-pass filtered, then sampled and stored on the Perkin-Elmer minicomputer for later processing.